This document is the Accepted Manuscript version of a Published Work that appeared in final form in The Journal of Physical Chemistry B, Copyright © 2021 The Authors. Published by American Chemical Society after peer review and technical editing by the publisher. To access the final edited and published work see https://pubs.acs.org/doi/10.1021/acs.jpcb.0c10311

Modeling and simulation of the aggregation and the structural and mechanical properties of silica aerogels

Rasul Abdusalamov,[*,†] Christian Scherdel,[‡] Mikhail Itskov,[†] Barbara Milow,[¶] Gudrun Reichenauer,[‡] and Ameya Rege[*,¶]

†*Department of Continuum Mechanics, RWTH Aachen University, Eilfschornsteinstr. 18, 52062 Aachen, Germany*

‡*Division Energy Efficiency, Bavarian Center for Applied Energy Research, Magdalene-Schoch Strasse 3, 97074 Würzburg, Germany*

¶*Department of Aerogels and Aerogel Composites, Institute of Materials Research, German Aerospace Center, Linder Höhe, 51147 Cologne, Germany*

E-mail: abdusalamov@km.rwth-aachen.de; ameya.rege@dlr.de

Abstract

Mechanical properties of aerogels are controlled by the connectivity of their network. In this paper, in order to study these properties, computational models of silica aerogels with different morphological entities have been generated by means of the diffusion-limited cluster-cluster aggregation (DLCA) algorithm. New insights into the influence of the model parameters on the generated aerogel structures and on the finite deformation under mechanical loads are provided. First, the structural and fractal properties of the modeled aerogels are investigated. The dependence of morphological properties such as the particle radius and density on these properties is studied. The results are correlated with experimental small angle X-ray scattering (SAXS) data of a silica aerogel. The DLCA models of silica aerogels are analyzed for their mechanical properties with finite element simulations. There, the aerogel particles are modeled as nodes, and the inter-particle bonds as beam elements to account for bond stretching, bending and torsion. The scaling relation between the elastic modululi E and relative density ρ, $E \propto \rho^m$ is investigated and the exponent $m = 3.61$ is determined. Backbone paths appear evidently in the 3-d network structure under deformation, while the majority of the bonds in the network do not bear loads. The sensitivity of particle neck-sizes on the mechanical properties is also studied. All the results are shown to be qualitatively as well as quantitatively in agreement with experimental data or with available literature.

Introduction

Classical supercritically dried silica aerogels are typically characterized by very low densities (around 100 kg m^{-3}) corresponding to high porosities around 95%.[1] In combination with typical pore sizes below 100 nm, silica aerogels have attracted considerable attention, specifically for thermal insulation applications, but also for cosmic dust capture and drug delivery[2,3] to name a few. There is considerable literature on the structural and mechanical properties of silica aerogels.[1,4–13] Most of these reports are experimental in nature while only very few theoretical investigations have been thus far reported. Silica aerogels deform

elastically under small strains, however under large strains, they undergo irreversible plastic deformation. Mechanical properties of the aerogels are often expressed by means of a power-law in terms of their density. The most commonly used power-law relation between the elastic modulus (E) and the relative density (ρ) is expressed as

$$E \propto \rho^m, \tag{1}$$

where m is the scaling exponent. Based on the open-cell foam model by Gibson and Ashby,[14] $m = 2$. However, aerogels exhibit random network connectivity, and do not boast a perfectly (fully) connected network structure which is the basis of the open-cell foam model. For this class of materials, the value of m lies between 2 and 4, as shown by, e.g., Groß and Fricke.[6] The effect of the density on the mechanical properties and behavior of silica aerogels was further investigated by Wong et al.,[10] who showed that the higher the density of the aerogels, the more brittle are their properties. An interesting feature of silica aerogels is their fractal nature. Being homogeneous on the macro scale, aerogels are known to have mass distributions that are fractal over certain length scales resulting from the aggregation of primary particles. Their fractal nature can be determined from small angle X-ray scattering (SAXS) or small angle neutron scattering (SANS) experiments. The scattering curves demonstrate three distinct regimes. Amongst these, in the intermediate regime, the slope of the double log plot of the scattering curve provides the fractal dimension directly.

Computational modeling has played a key role in investigating the mechanical and fractal features of aerogels. Different modeling tools applied in this context include molecular dynamics simulations,[12,15,16] coarse-grained hard-sphere aggregation approaches,[11,17–20] flexible coarse-grained approaches,[21–23] constitutive models,[24] and multiscale models.[25] Silica aerogels are synthesised by means of the sol-gel process. This involves the assembly of small particles to form clusters and networks. Such a process can be modeled by means of the aggregation mechanism. There are several particle-based aggregation algorithms, e.g., diffusion limited aggregation (DLA), reaction-limited aggregation (RLA), diffusion-limited cluster(-

cluster) aggregation (DLCA), reaction-limited cluster(-cluster) aggregation (RLCA), ballistic, etc. Hasmy et al.[17,18] investigated the application of the above mentioned algorithms to model silica aerogels. Accordingly, the shape of the experimental scattering curve is qualitatively well reproduced by cluster-cluster algorithms. They modeled silica aerogels by means of DLCA on the basis of the work by Kolb and Herrmann.[26] Ma et al.[11,19,20] further extended their approach to describe the bulk mechanical properties of silica aerogels and investigate the effect of dangling bonds on the network behavior. Accordingly, the dangling mass does not represent a key factor for determining the scaling exponent. They studied the density dependence on the bulk modulus by subjecting the DLCA networks under hydrostatic compression. While the above-mentioned works used unit diameters to model the particles, Haard et al.,[27] applied a log-normal and a truncated Gaussian distribution function for the particle radius, based on the interpretations from the experimental data. Even though previous studies have attempted to characterize silica aerogels by means of the DLCA, there is no clear consensus on the effect of different model parameters on the generated morphology as well as on the finite deformation under mechanical loads. To the best of our knowledge, the three-dimensional (3-d) network modeling of silica aerogels, along with a subsequent analysis under finite deformations have not been reported in this detail. Thus, this study aims at analyzing different model parameters and their effect on the structural and fractal properties of silica aerogels. Furthermore, finite deformations are considered in order to understand the role of network connectivity on the load-transfer-path as well as to describe the bulk mechanical properties of silica aerogels.

The paper is organized as follows. In section Methods, the detailed methodology of DLCA modeling of silica aeorgels and the subsequent finite element modeling. More information about the application of periodic boundary conditions in the finite element model is also provided in the appendix A. In section Results and Discussion, the structural and fractal features of the silica aerogel models obtained by means of the DLCA modeling are elucidated. Finally, the mechanical properties and the influence of different morphological parameters

on them are described. The synthesis and characterization of silica aerogels is outlined in appendix B.

Methods

DLCA model

Several aggregation algorithms can model particles undergoing random walks due to Brownian motion and the formation of clusters that in turn form aggregates making up the network. The sol-gel process used to synthesize silica aerogels follows a similar process of clustering. Since Hasmy et al.[17] showed that the structures obtained from the diffusion limited cluster-cluster aggregation (DLCA) best agree with the scattering data of silica aerogels, and since Ma et al.[11] played down the significance of the choice of a particular aggregation algorithm, the DLCA algorithm was applied in this work to model silica aerogel networks. The methodology of the algorithm is described as follows.

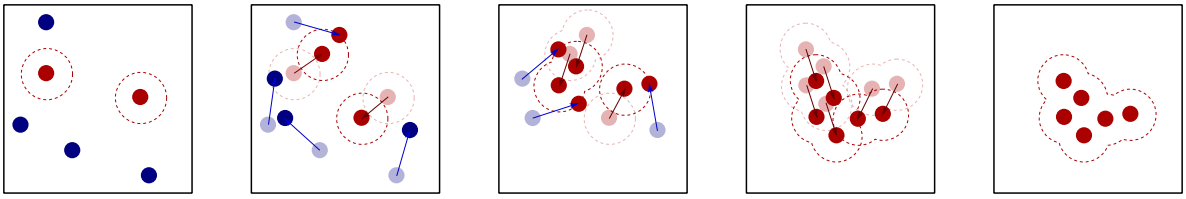

(a) Time step 1 (b) Time step 2 (c) Time step 3 (d) Time step 4 (e) Time step 5

Figure 1: Illustration of the off-lattice DLCA algorithm in 2-d: seeds visualized in red and walkers in blue. Through time all walker particles are connected to the seeds and clusters are formed (transparent particles show the previous position). The model and all subsequent simulations in this study are based on an off-lattice 3-d DLCA model.

In order to model the microstructure of silica aergoels, the DLCA method was utilized. The algorithm is explained below and illustrated in Fig. 1. As a starting point for the method, a box with periodic boundary conditions has to be defined. Within this box a total number $N_{\text{all}} = N_{\text{S}} + N_{\text{W}}$ of seeds and walker particles are initialized (see Fig. 1a). These can be placed randomly or in an arranged way within the box. In this illustrative example,

the particles were placed at random points and were then allowed to move freely according to the random walk theory. For this purpose, a seed and walker step size was initialized (visualized as arrows in Fig 1). Note that for simplicity purposes, Fig. 1 shows a scheme for the off-lattice algorithm in 2-d although it was implemented in 3-d. The off-lattice algorithm required defining a critical distance $\varepsilon_{\text{crit}}$ from a walker to a seed particle (see red dotted circles around seeds). As soon as it was reached, the Brownian motion was stopped and the walker diffused to the seed, binding to it. Additionally, a sticking probability p_s was defined to model the cluster diffusion. Here, we set the sticking probability $p_s = 1$, i.e., the walker particles always stick once the critical distance is reached. With time, all the walkers diffuse to the seeds and clusters are formed (see Fig. 1b and 1c). As soon as two particles of two different clusters likewise exceed this critical distance $\varepsilon_{\text{crit}}$, the two clusters are connected to form one single cluster[11] (Fig. 1d and 1e). Hence, the term cluster-cluster aggregation is used based on the ideas presented by Meakin.[28] The movement of the clusters (seeds) was slower than the movement of the walkers. All particles continue to move until all walkers are connected in a cluster and all clusters are connected to each other. In this particular work, the particles move continuously in space. Thus, a total of seven inputs were varied: the radius of particles r, the critical distance $\varepsilon_{\text{crit}}$, the number of walkers N_{W}, the number of seeds N_{S} , the seed step s_{S}, the walker step s_{W} and the box size L. In principle, more parameters, e.g., the sticking probability and the type of motion, can also be varied. An object-oriented approach was used for the implementation in MATLAB.

Silica aerogels are very good examples of fractal materials such that computationally generated and chemically synthesized structures can be correlated by comparing their fractal properties. The latter can be quantified by the fractal dimension d_{f}, which is a parameter that characterizes the geometric properties of a structure by describing the self similarity of a structure on a particular length scale. There are several methods to calculate d_{f}. One of them is to determine the mass $m(r)$ of the particles inside a sphere of radius r. The radius of the sphere is first varied, and then the logarithmic increase of $m(r)$ is recorded.

The relationship between $m(r)$ and r demonstrates a power law $m(r) \propto r^{d_\mathrm{f}}$, where the slope of the resulting curve (plotted on a log-log scale) corresponds to the exponent d_f, which is the fractal dimension. Once the fractal dimension is determined for a given density of silica aerogel, it is correlated to the value obtained from experimental curves of SAXS. The influence of the relative density on the fractal dimension is further investigated. To this end, silica aerogel structures with relative densities $\rho \in [0.03, 0.1]$ were generated and the fractal dimensions were measured. Exemplarily, 3-d structures of silica aerogels with different densities $\rho = 0.03, 0.045$ and 0.06, are illustrated in Fig. 2 (a), (b) and (c), respectively. Fig. 2 (d) shows a 2-d cross-section of the middle frame of the 3-d simulation box illustrating random network connectivity and high porosity within the network. A few particles appear to be unconnected and isolated in the simulation box. However, these were connected to other particles of the clusters *via* periodic boundary conditions. It was made sure that all particles and clusters in the simulation box were connected to the backbone by the end of the simulation, as would be the case in a silica aerogel precursor for long gelation/aging times. Fig. 2 (e) schematically illustrates a completely connected network. Moreover, the influence of the particle radius on the fractal dimension was determined. This was done by varying only the particle radius and keeping all other variables constant. For each radius, a total of 10 simulations were performed and the results were averaged. A simulation box with the edge length $L = 200\,\mathrm{nm}$ was chosen. The average particle radius as determined by the SAXS measurements was 3.1 nm. The number of particles N_tot were subsequently determined from the given relative density ρ. Besides the radius and the edge length, the step size of the seed and walker particles can be defined, which in this case were specified to be $2s_\mathrm{s} = s_\mathrm{w} = {}^{R}/_{10}$.

Finite Element Model

In order to describe the mechanical properties of the generated aggregates, the finite element method (FEM) was utilized. Given the geometry of the structures, the information about all particle positions and all connections between the particles was known *a priori*. In

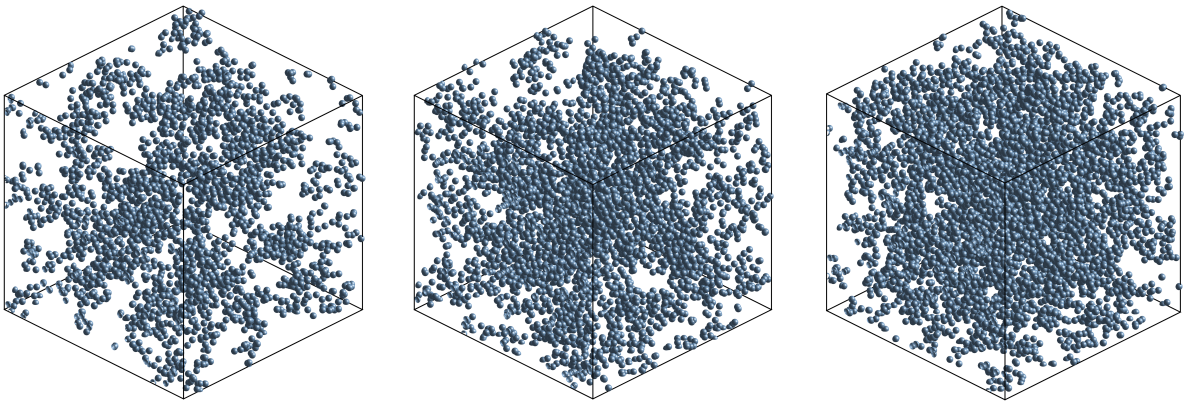

(a) $\rho = 0.03$ (b) $\rho = 0.045$ (c) $\rho = 0.06$

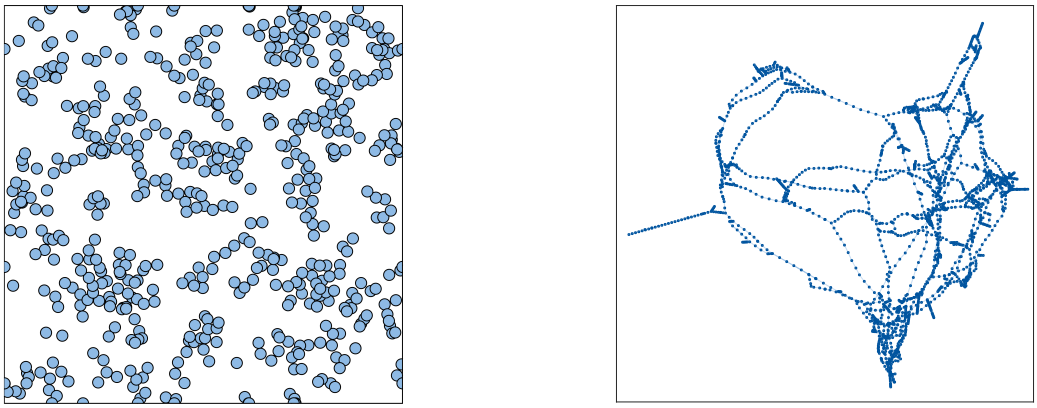

(d) Cross section for $\rho = 0.06$ (e) Graph plot for $\rho = 0.06$

Figure 2: (a)-(c) Illustration of the generated aerogel structure with DLCA for different relative densities. The low porosity of the structures is clearly visible. The cross section in (d) was generated by cutting out a slice in the middle of simulation box at $x = 100\,\text{nm}$ with a width of $w = 4R$. (e) Graph plot of the 3-d backbone illustrating the fully connected network, by means of 2-d projections.

order to perform a FEM simulation, a representative volume element (RVE) was created. Its dimensions corresponded to the dimensions of the DLCA simulation box. Additionally, periodic boundary conditions were considered in order to model the whole structure by simulating only the RVE. While implementing the DLCA algorithm, the boundary surfaces of the box were subjected to periodic boundary conditions. However, this alone does not guarantee the presence of particles on the boundary. In order to generate periodic nodes, any connection between two particles that crosses a boundary surface was filtered. For each node on a boundary surface the complementary node on the complementary surface was created.

Each particle connection was separated exactly on the surface by the boundary surface and a new node was subsequently created. These new nodes were stored in a special set of periodic boundary nodes. The old particle connection was deleted and two new connections with the intermediate node on the boundary surface were created. Thus, the periodic boundary conditions were applied to the newly generated node as described in Appendix B.

The particles from the DLCA structure were modeled as nodes while the connections (bonds) were modeled as beams. The FEM program ABAQUS was used, and the beam element type B31 based on the Timoshenko beam theory was applied. Beam elements were used because they reflect all three deformation modes of a bond, which are bending, torsion and stretching. Young's modulus and Poisson ratio of the beams were specified as $E = 10^5\,\mathrm{Pa}$ and $\nu = 0.29$, respectively.[11] A point at the center of the RVE was fixed, so that the RVE is expanded or compressed about the center. Moreover, to avoid penetration between all beams, frictionless contact was defined. However, self contact between each beam element was excluded. To perform the simulations input decks were created by a function in MATLAB. The RVEs were subjected to uniaxial compression, which is the common mode of deformation used to analyze the mechanical properties of silica aerogels.

The aerogel RVEs with different relative densities were simulated. Aging of aerogels has shown to influence the neck-growth between the particles in the aerogel network.[29,30] Within a finite element framework, the neck-growth is modeled as the growth in the bond (beam) diameter d_{bond}, and its influence on the elastic modulus of the network was studied.

Results and discussion

DLCA model evaluation

The presented model structures in Figs. 2 (a)-(c) exhibited grossly similar characteristics to those of silica aerogels. To quantify the relative density of the generated structures, the

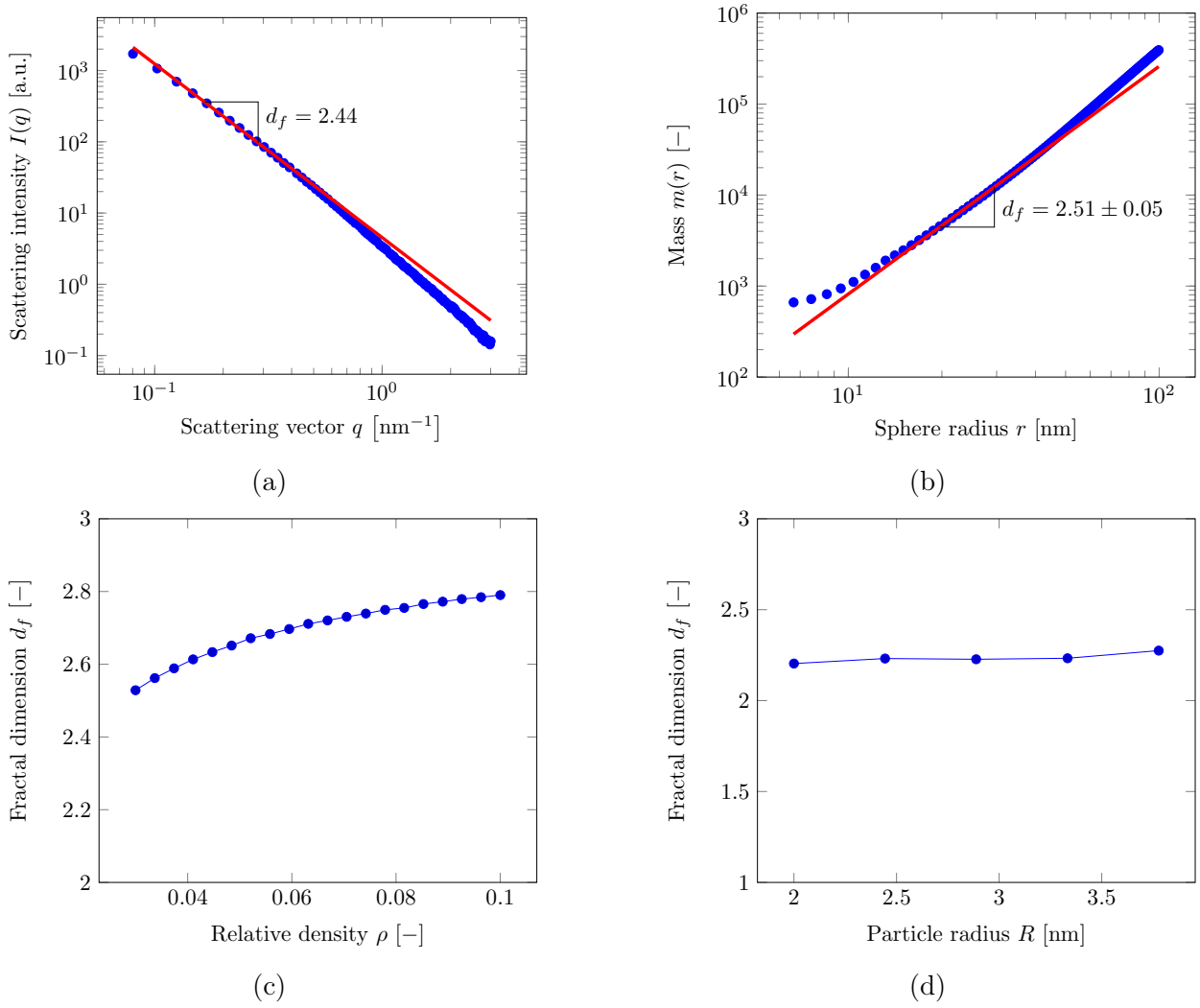

Figure 3: (a) Scattering curve of the wet silica gel synthesized with a pH of 7.0 that shows the fractal slope $d_f = 2.44$ and the subsequent transition to the Porod behavior, (b) determination of the fractal dimension by determining the mass $m(r)$ inside a sphere with radius r, (c) influence of the relative density on the fractal dimension, (d) influence of the particle radius on the fractal dimension.

volume of all particles V_p in ratio to the volume V_b of the simulation box was calculated by

$$\rho = \frac{V_\mathrm{p}}{V_\mathrm{b}} = \frac{4\pi N_\mathrm{all} R^3}{3L^3}, \tag{2}$$

where R denotes the particle radius and L is the box size. The porosity, evaluated as $\phi = 1 - \rho$ for the generated structures with different relative densities was in agreement with

the corresponding values of the synthesized aerogels. The mass fractal dimensions were first evaluated for different values of ρ as a function of distance r from the reference point inside the aggregate. The ratio is expressed as $m(r) \propto r^{d_\mathrm{f}}$, where $0 < d_\mathrm{f} < 3$ is the fractal dimension of the aggregate. For example, a structure with particle-size and density corresponding to the experimentally synthesized wet gel with a pH=7.0 was generated and investigated for the fractal properties. The scattering curve of the wet silica gel in Fig. 3 (a) shows a fractal slope with $d_f = 2.44$ at q-values between 0.12 nm^{-1} and 0.45 nm^{-1}. For more details on the synthesis and characterization of the silica aerogel, refer to Appendix B. Fig. 3 (b) shows the computationally obtained value of d_f=2.51 $\pm$ 0.05. This agreed well with the experimentally determined value of 2.44.

The influence of the relative density on the fractal dimension was further investigated. The relative density depends on three different inputs, however, only the number of particles was varied because the ratio between the box size length and the radius is scalable and would have no effect on the fractal dimension. Fig. 3 (c) shows that d_f increased slightly with the increasing relative density of the silica aerogel network. Within the range of slight increase, the increment was stronger for low-density aerogels and softer for higher density ones (beyond ρ=0.06). This agreed well with MD simulations.[13,16,31] Next, the influence of particle-sizes on d_f was investigated and is shown in Fig. 3 (d). Note that the size of the simulation box varied with the changing particle radii, thus preserving the relative density. It can be realized that varying only the particle radius by keeping all other model parameters constant showed no influence on d_f. Hence, the approach used by Hasmy et al.[18] and Ma et al.[11] of using a constant particle radius was chosen over the one by Haard et al.[27] of using a size distribution, because the particle radius had no influence on the fractal properties of the aerogels. However, unlike the other works,[11,18] the numerical value of the particle radius was chosen from experiments, and not just as a unit value.

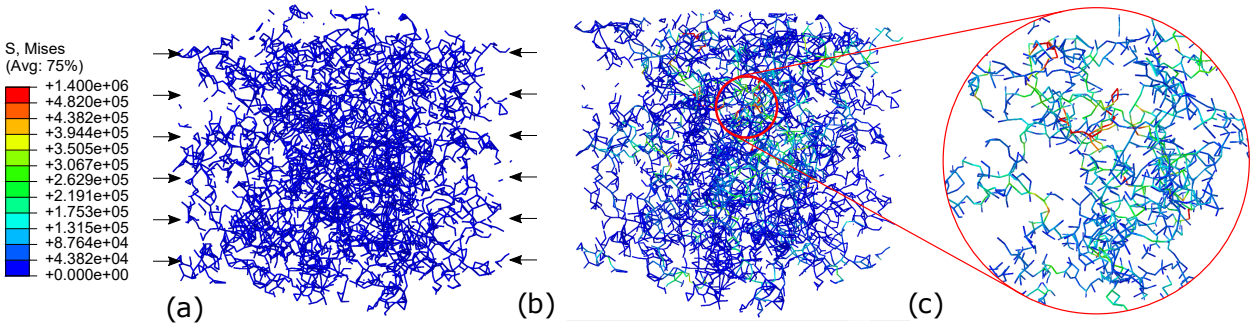

Figure 4: FE simulation of the silica aerogel RVE: Visualization of von Mises stresses under the applied uniaxial compression of 10% (a) reference, (b) deformed state, (c) zoomed image under deformed state showing the critical backbone path of the load transmission.

Investigation of the mechanical properties

The above-investigated DLCA structures were then exported into the finite element program ABAQUS as described in the Methods section and were subjected to compression. In Figs. 4 (a) and (b), the reference and deformed states of the RVE are shown, respectively. The network was seen as mostly perfectly connected. Nevertheless, under compression of the structure, not all its bonds appeared to be loaded. Very few backbone paths appeared to bear the load that the complete network was subjected to (see Fig. 4 (c) which shows the zoomed visualization of the backbone path), while the majority of the bonds were stress-free. Note also that this was the case for all simulated densities. Ferreiro-Rangel and Gelb[23] reported in their coarse-grained simulation study, that less than 1% of bonds were broken at maximum tensile stress. Also, previous studies[11] have reported that in the case of silica aerogels, at the most 10% of the bonds would actually bear the total load subjected to the entire 3-d network. Figs. 4 (b) and (c) not only demonstrate such an effect, but rather show the appearance of the backbone paths. The term backbone appears from colloidal mechanics where it is used to identify the shortest stress path which bears the majority of load within the colloidal network structure. This shows that the network connectivity, and not just the density, is the key player in determining the mechanical properties of the aerogels.

To quantify the mechanical properties, the elastic modulus E of the network was obtained from the stress-strain curves under uniaxial compression. E is plotted against the different

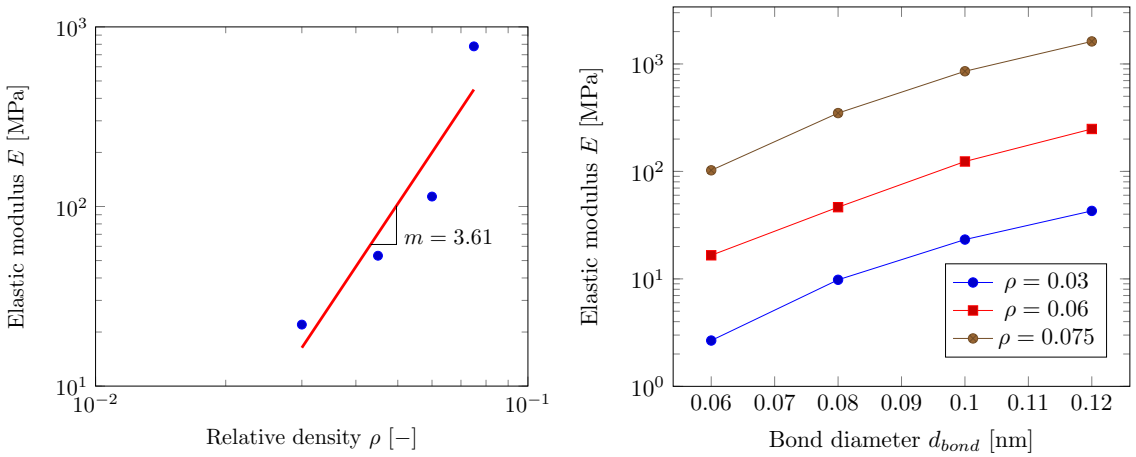

Figure 5: a) Log-log plot of the elastic modulus E vs. the relative density ρ, b) E vs. d_{bond}.

simulated relative densities ρ in Fig. 5 (a). The scaling exponent m from the power law expression in Eq. (1) is evaluated to be 3.61. This value is comparable and even in good agreement with other modeling studies and experimental values (see Table 1). It was also of interest to quantify the effect of the particle neck-sizes on the elastic modulus. To model this morphological effect, the diameter of the beam (bond) d_{bond} between the particles was varied. For a constant relative density, the effect of varying d_{bond} on the elastic modulus of the aerogel network structure is plotted in Fig. 5 (b). The stiffness of the network increased with d_{bond}, but this increase flattened with larger values of d_{bond}. It was realized that increasing the neck-size three-four times resulted in a two orders of magnitude stiffer network response. This was in agreement with the experimental work by Einarsrud et al.,[29,30] where mechanical strengthening of silica aerogels was achieved by increasing the neck-sizes by means of aging.

Conclusions

The application of the DLCA algorithm was shown to be effective in modeling and interpreting the structural and fractal features of silica aerogels. The influence of morphological entities, such as the density and particle radii, on the fractal dimension was investigated. While the fractal dimensions show a slight non-linear increase with the relative density, the

Table 1: Comparison of the scaling exponent m obtained in our work vs. those from other modeling and experimental works. CG: coarse-grained modeling, MD: molecular dynamics simulations.

Work	**Method**	**Exponent m**
Modeling		
Rivas-Murillo et al.[16]	MD	3.11 ± 0.21
Ferreiro-Rangel and Gelb[23]	CG	3.0 ± 0.2
Patil et al.[12]	MD	3.25 ± 0.1
Gonçalves et al.[13]	MD	3.84 ± 0.22
Our work	DLCA+FEM	3.61
Experimental		
Woignier et al.[32]	SiO_2 aerogels	3.7 ± 0.2
Groß and Fricke[6]	SiO_2 aerogels	3.49 ± 0.07
Groß and Fricke[6]	sintered SiO_2 aerogels	2.97 ± 0.05

increase in particle-sizes within the clusters shows no influence on the fractal dimensions. As minor fluctuations in the particle diameter did not significantly change the properties, a monomodal particle size distribution was sufficient. The calculated values of the fractal dimensions as obtained from the model structures were shown to correspond to those estimated from the SAXS curves.

The implementation of the DLCA-generated aerogel structures in a finite element model made it possible to evaluate the mechanical properties of the aerogels. By means of stress contour diagrams and strain energy visualizations of the 3-d structures under deformation, it was realized that majority of the bonds within the network do not bear any mechanical load. The appearance of the critical load (backbone) path could be explicitly visualized, a first for a simulation-based study on silica aerogels. The elastic modulus was shown to scale with the relative density according to the power scaling law with the exponent value of 3.61. Finally, the influence of thicker particle necks on the elastic modulus was analyzed. While an increasing trend was found throughout, the increase was shown to saturate for higher values of the neck-size. The proposed modeling approach presents a framework for further investigating the pore collapse and densification in the silica aerogel network.

Appendix

A: Application of periodic boundary conditions

Each node has 6 degrees of freedom, three translational and three rotational. Additionally, the degrees of freedom at the box boundaries are coupled by periodic boundary conditions using dummy nodes. Therefore three dummy nodes $\boldsymbol{X}^A$, $\boldsymbol{X}^B$ and $\boldsymbol{X}^C$ are defined. Each node corresponds to a surface pair of the box, e.g. $\boldsymbol{X}^A$ couples all degrees of freedom on the left and right surface of the box. With $\boldsymbol{\theta} = \begin{pmatrix} x & y & z & \phi_x & \phi_y & \phi_z \end{pmatrix}^\top$ representing the degrees of freedom the coupling conditions are given by:

$$\begin{aligned} \boldsymbol{\theta}^{\text{left}} - \boldsymbol{\theta}^{\text{right}} &= \boldsymbol{X}^A \\ \boldsymbol{\theta}^{\text{top}} - \boldsymbol{\theta}^{\text{bottom}} &= \boldsymbol{X}^B \\ \boldsymbol{\theta}^{\text{front}} - \boldsymbol{\theta}^{\text{back}} &= \boldsymbol{X}^C \ . \end{aligned}$$

These conditions are implemented as `*Equations` in ABAQUS.

B: Synthesis and characterization of silica aerogels

Synthesis

The silica aerogel was synthesized according to the recipe by Reichenauer.[33] The synthesis parameters of the 1-step base-catalyzed silica gel are: target density 100 kg m^{-3} and a 4.0 molar ratio of water to TMOS. No base or acid was added, thus the pH of the solution was assumed to be 7.0. After stirring, the sol was filled into cylindrical moulds, left for 5 days at 30 °C for gelling and ageing. After removal from the moulds, the silica gel was washed 2 times with ethanol prior to characterization with SAXS in order to obtain a well-defined pore liquid and to stop ageing reactions due to remaining water in the pores.

Characterization

The SAXS characterization was performed with a SAXSpoint 1.0 instrument from Anton Paar using Cu K_α radiation (wave length 1.54 Å) and a sample detector distance of 582 mm. For the measurements, the wet gel was placed into a sealed cell with polyimide windows and an excess of ethanol to avoid drying. After measurement, the scattering of ethanol was subtracted manually from the scattering curve of the wet gel. In the fractal region of the scattering curve, a power law $I(q) \sim q^{-d_\mathrm{f}}$ was fitted to derive the fractal dimension d_f of the wet sample for comparison with the simulation. The scattering curve of the wet silica gel in Fig. 3 (a) shows a fractal slope with $d_\mathrm{f} = 2.44$ at q-values between 0.12 nm^{-1} and 0.45 nm^{-1}. For scattering vectors q > 2 nm^{-1} the slope moves towards Porod behavior, (i.e. $I(q) \sim q^{-4}$) of the scattering from its smooth interface. At small q-values, the flattening of the scattering curve is related to the cluster size originating from the aggregation mechanism of the particles, e.g., by DLCA.

References

(1) Gross, J.; Reichenauer, G.; Fricke, J. Mechanical properties of SiO2 aerogels. *Journal of Physics D: Applied Physics* **1988**, *21*, 1447–1451.

(2) Hrubesh, L. W. Aerogel applications. *Journal of Non-Crystalline Solids* **1998**, *225*, 335–342.

(3) Smirnova, I.; Suttiruengwong, S.; Arlt, W. Feasibility study of hydrophilic and hydrophobic silica aerogels as drug delivery systems. *Journal of Non-Crystalline Solids* **2004**, *350*, 54–60.

(4) Gross, J.; Fricke, J.; Pekala, R. W.; Hrubesh, L. W. Elastic nonlinearity of aerogels. *Phys Rev B Condens Matter* **1992**, *45*, 12774–12777.

(5) Gross, J.; Fricke, J. Ultrasonic velocity measurements in silica, carbon and organic aerogels. *Journal of Non-Crystalline Solids* **1992**, *145*, 217–222.

(6) Groß, J.; Fricke, J. Scaling of elastic properties in highly porous nanostructured aerogels. *NanoStructured Materials* **1995**, *6*, 905–908.

(7) Parmenter, K. E.; Milstein, F. Mechanical properties of silica aerogels. *Journal of Non-Crystalline Solids* **1998**, *223*, 179–189.

(8) Reichenauer, G. *Aerogels Handbook*; Springer, 2011; pp 449–498.

(9) Maleki, H.; Durães, L.; Portugal, A. An overview on silica aerogels synthesis and different mechanical reinforcing strategies. *Journal of Non-Crystalline Solids* **2014**, *385*, 55–74.

(10) Wong, J. C.; Kaymak, H.; Brunner, S.; Koebel, M. M. Mechanical properties of monolithic silica aerogels made from polyethoxydisiloxanes. *Microporous and mesoporous materials* **2014**, *183*, 23–29.

(11) Ma, H.-S.; Roberts, A. P.; Prévost, J.-H.; Jullien, R.; Scherer, G. W. Mechanical structure-property relationship of aerogels. *Journal of Non-Crystalline Solids* **2000**, *277*, 127–141.

(12) Patil, S. P.; Rege, A.; Sagardas,; Itskov, M.; Markert, B. Mechanics of Nanostructured Porous Silica Aerogel Resulting from Molecular Dynamics Simulations. *The Journal of Physical Chemistry B* **2017**, *121*, 5660–5668.

(13) Gonçalves, W.; Morthomas, J.; Chantrenne, P.; Perez, M.; Foray, G.; Martin, C. L. Elasticity and strength of silica aerogels: A molecular dynamics study on large volumes. *Acta Materialia* **2018**, *145*, 165–174.

(14) Gibson, L. J.; Ashby, M. F. *Cellular solids: structure and properties*; Cambridge university press, 1999.

(15) Pohl, P. I.; Faulon, J.-L.; Smith, D. M. Molecular dynamics computer simulations of silica aerogels. *Journal of non-crystalline solids* **1995**, *186*, 349–355.

(16) Rivas Murillo, J. S.; Bachlechner, M. E.; Campo, F. A.; Barbero, E. J. Structure and mechanical properties of silica aerogels and xerogels modeled by molecular dynamics simulation. *Journal of Non-Crystalline Solids* **2010**, *356*, 1325–1331.

(17) Hasmy, A.; Foret, M.; Pelous, J.; Jullien, R. Small-angle neutron-scattering investigation of short-range correlations in fractal aerogels: Simulations and experiments. *Phys Rev B Condens Matter* **1993**, *48*, 9345–9353.

(18) Hasmy, A.; Anglaret, E.; Foret, M.; Pelous, J.; Jullien, R. Small-angle neutron-scattering investigation of long-range correlations in silica aerogels: Simulations and experiments. *Physical Review B* **1994**, *50*, 6006–6016.

(19) Ma, H.-S.; Prévost, J.-H.; Jullien, R.; Scherer, G. W. Computer simulation of mechanical structure-property. *Journal of Non-Crystalline Solids* **2001**, *285*, 216–221.

(20) Ma, H.-S.; Prévost, J.-H.; Scherer, G. W. Elasticity of DLCA model gels with loops. *International Journal of Solids and Structures* **2002**, *39*, 4605–4614.

(21) Gelb, L. D. Simulating Silica Aerogels with a Coarse-Grained Flexible Model and Langevin Dynamics. *The Journal of Physical Chemistry C* **2007**, *111*, 15792–15802.

(22) Ferreiro-Rangel, C. A.; Gelb, L. D. Investigation of the bulk modulus of silica aerogel using molecular dynamics simulations of a coarse-grained model. *The Journal of Physical Chemistry B* **2013**, *117*, 7095–7105.

(23) Ferreiro-Rangel, C. A.; Gelb, L. D. Computational study of uniaxial deformations in silica aerogel using a coarse-grained model. *The Journal of Physical Chemistry B* **2015**, *119*, 8640–8650.

(24) Lei, J.; Liu, Z. A novel constitutive model for the mechanical properties of silica aerogels. *Journal of Applied Physics* **2018**, *124*.

(25) Rege, A.; Patil, S. P. On the Molecular to Continuum Modeling of Fiber-Reinforced Composites. *Advanced Theory and Simulations* **2020**, *3*, 1900211.

(26) Kolb, M.; Herrmann, H. J. The sol-gel transition modelled by irreversible aggregation of clusters. *Journal of Physics A* **1985**, *18*, L435–L441.

(27) Haard, T. M.; Gervais, G.; Nomura, R.; Halpern, W. P. The pathlength distribution of simulated aerogels. *Physica B: Condensed Matter* **2000**, *284-288*, 289–290.

(28) Meakin, P. Diffusion-limited aggregation in three dimensions: Results from a new cluster-cluster aggregation model. *Journal of Colloid and Interface Science* **1984**, *102*, 491–504.

(29) Einarsrud, M.-A.; Nilsen, E. Strengthening of water glass and colloidal sol based silica gels by aging in TEOS. *Journal of Non-Crystalline Solids* **1998**, *226*, 122–128.

(30) Einarsrud, M.-A.; Nilsen, E.; Rigacci, A.; Pajonk, G. M.; Buathier, S.; Valette, D.; Durant, M.; Chevalier, B.; Nitz, P.; Ehrburger-Dolle, F. Strengthening of silica gels and aerogels by washing and aging processes. *Journal of Non-Crystalline Solids* **2001**, *285*, 1–7.

(31) Kieffer, J.; Angell, A. Generation of fractal structures by negative pressure rupturing of SiO2 glass. *Journal of Non-Crystalline Solids* **1988**, *106*, 336–342.

(32) Woignier, T.; Phalippou, J.; Vacher, R. Parameters affecting elastic properties of silica aerogels. *Journal of Materials Research* **1989**, *4*, 688–692.

(33) Reichenauer, G. Thermal aging of silica gels in water. *Journal of Non-Crystalline Solids* **2004**, *350*, 189–195.

Graphical TOC Entry